AGE ESTIMATES OF GEOLOGIC UNITS AROUND THE REMBRANDT BASIN, MERCURY.

J. Gemperline[1-2], B. M. Hynek[1-2], S. J. Robbins[3], M. K. Osterloo[1], K. Mueller[2], R. Thomas[1], [1]Laboratory for Atmospheric and Space Physics & [2] Dept. of Geological Sciences, University of Colorado-Boulder, Campus Box 600 UCB, Boulder, CO 80303, [3]Southwest Research Institute, 1050 Walnut St., Suite 300, Boulder, CO 80302. John.Gemperline@lasp.colorado.edu

Introduction: A complete draft of geologic units, contacts, linear features, and surface features has been compiled and previously reported in order to understand the geological history of Rembrandt basin and thus interpret the evolution of Mercury at a regional and global scale [1]. Relative and absolute age estimates based on crater statistics provide an additional means of determining timing of formation along with stratigraphic and cross-cutting relationships. Based on previous crater studies using MESSENGER data [2,3], secondary craters may be a significant issue in our mapping region for craters as large as $D = 10$ km. A comprehensive analysis of primary craters that pre- and post-date the units in this region will also help determine the role of resurfacing events and the possible influence of layering on the formation of the present surface.

Methods: We created custom controlled mosaics at 100 m/pix from ~2600 NAC images, filtered by incidence angle (60°-70°; 70°-80°; 80°-90°), to highlight topographic features including crater rims, peaks, and ejecta [1]. These were used to generate a database of 47,032 craters in the range ~0.5-190 km in the study region, based on the methods in Robbins and Hynek, 2012 [4]. This comprehensive crater database spanning 4% of Mercury's surface allows us to create reasonable age estimates.

Obvious secondary craters were classified based on morphologic properties including clustering, emplacement in chains, herringbone ejecta patterns, and/or high ellipticity with a shallow half pointing radially from a larger crater. In total, 29,863 secondary craters were identified (representing 63.5% of the crater total) and excluded from the population used for stratigraphic and modeled crater ages.

We used several different production functions within the Craterstats2 software [5] to produce relative and absolute age estimates from the remaining population of 17,169 primary craters. Craters ≥40 km in diameter that were originally mapped as separate geologic units were re-mapped to be included within the underlying unit on which they formed (**Fig. 1**).

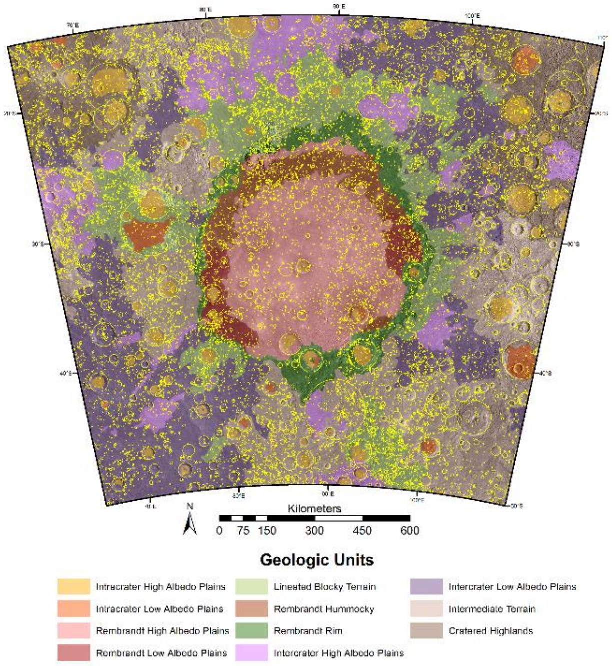

Figure 1: Rembrandt Basin mapping area with geologic units used for crater counting. Primary crater rims are highlighted in yellow.

Absolute model ages (AMAs) were calculated for nine geologic units: Intercrater High Albedo Plains (IeHP), Intercrater Low Albedo Plains (IeLP), Intermediate Terrain (IT), Cratered Highlands (CH), Rembrandt High Albedo Plains (RHP), Rembrandt Low Albedo Plains (RLP), Lineated Blocky Terrain (LBT), Rembrandt Hummocky (RH), and Rembrandt Rim (RR). Intracrater High Albedo Plains (IaHP) and Intracrater Low Albedo Plains (IaLP) were not included in this crater count and will be updated in the future. AMAs were calculated from the number of craters with diameter ≥5 km (**Table 1**) for the whole unit using the production and chronology functions from both the Neukum Production Function and chronology function (NPF) and Le Feuvre and Wieczorek model production Function and chronology function (LF&W) [6, 7]. For the LF&W, both non-porous and porous scaling laws for target materials were considered.

Table 1: Absolute model ages for D≥5 km with statistical uncertainties.

Unit	NPF	LF&W (non-porous)	LF&W (porous)	# of craters
IeHP	4.0 ± 0.0	3.7 ± 0.0	3.8 ± 0.0	107
IeLP	4.0 ± 0.0	3.7 ± 0.0	3.8 ± 0.0	293
IT	4.0 ± 0.0	3.7 ± 0.0	3.9 ± 0.0	480
CH	4.0 ± 0.0	3.7 ± 0.0	3.8 ± 0.0	170
RHP	3.9 ± 0.0	3.6 ± 0.0	3.8 ± 0.0	104
RLP	4.0 ± 0.0	3.7 +0.0, -0.1	3.8 ± 0.0	20
LBT	4.0 ± 0.0	3.7 ± 0.0	3.8 ± 0.0	253
RH	4.0 ± 0.0	3.7 ± 0.0	3.8 ± 0.0	48
RR	4.0 ± 0.0	3.7 ± 0.0	3.8 ± 0.0	67

Discussion: Fitting AMAs to Hermean craters is a complicated task. Ideally, large craters would be used to avoid secondaries; however, using $D \geq 20$ km resulted in some units with just 1 crater and most <20, providing for poor number statistics. Using $D \geq 3$ km showed significant deviations from both model production functions. We found ≥5 km craters to be a reasonable compromise between these issues (*e.g.*, Fig. 2) and used CraterStats2 to calculate the AMAs. That our crater population reasonably follows the PFs is good evidence that we did a reasonable removal of the vast secondary crater population in this region.

Overall the NPF provides older ages than the LF&W of 4.0 Ga for all units except RHP. The LF&W porous scenario provides ages around 3.8 Ga for all of the units besides IT. The LF&W non-porous provides the youngest ages of 3.7 Ga excluding the RHP. Determining whether to use the porous or non-porous scenario is not possible without in situ data for the map area. However, integrating geologic heterogeneities over larger areas generally approximates the porous scenario.

The general trends in each scenario show the units to be clustered around one age indicating a relatively short emplacement time around or during the impact that formed Rembrandt Basin. Cratered Highlands are interpreted to be the oldest surface based on stratigraphic relationships and interpretation of the scalloped, heavily cratered surface. Ages calculated from the NPF and LF&W non-porous give CH an older age while the LF&W porous scenario shows CH to be younger than IT. This may be due to saturation at smaller crater diameters and difficulty in identifying crater rims from topography in highly degraded terrain. A further complication is attempting to differentiate between primary and secondary craters, especially considering many primary structures may have been erased by secondary impacts. IT is ascribed an older age, particularly in the porous LF&W scenario, suggesting the surface predates basin formation.

All units related to the formation of Rembrandt Basin match in age (between 3.8-4.0 Ga), with the exception of the RR being 0.1 Ga younger in the non-porous LF&W scenario. Using the LF&W porous scenario, this study puts the formation of Rembrandt at 3.8 Ga in agreement with previous work that dated the formation of Rembrandt to 3.8 ± 0.1 Ga [8]. These units would have formed rapidly and at approximately the same time. Steep scarps and limited area are both complicating factors in crater age estimation techniques, and both are characteristics of the RR unit, potentially providing an erroneously younger age. The RHP unit is ascribed a younger age by all three methods, in good agreement with an interpreted effusive volcanic infilling post-dating basin formation (**Figure 2**).

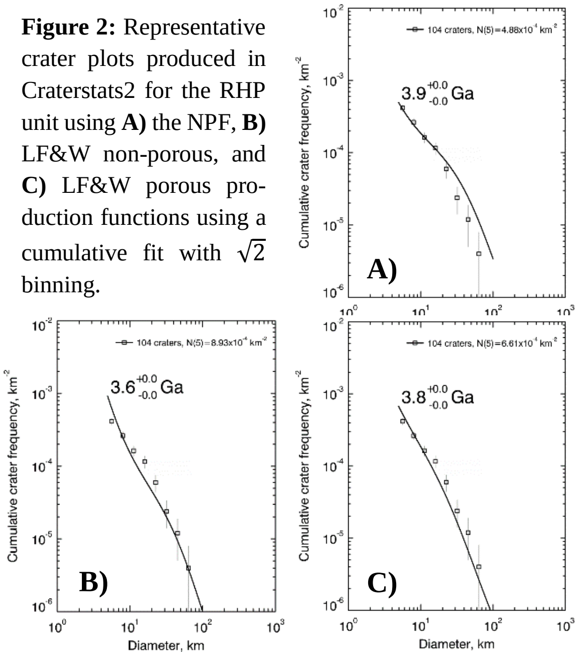

Figure 2: Representative crater plots produced in Craterstats2 for the RHP unit using **A)** the NPF, **B)** LF&W non-porous, and **C)** LF&W porous production functions using a cumulative fit with $\sqrt{2}$ binning.

Among the primary crater population in the study area, identifying pre- and post-dating craters by separating pristine, degraded, and partially buried craters has not yet been completed. While total crater statistics yield insights into emplacement ages, superposed craters indicate the ages of the most recent major resurfacing event or potential layering within target materials. Further efforts will focus on strictly homogenous target regions for each geologic unit to refine these age estimates. AMAs produced with other production functions will also be obtained and compared to those produced here.

Acknowledgements: Funding for this work came from NASA PGG grant NNX14AP51G.

References: [1] Hynek, B.M. et al., (2016) *47th LPSC*, abstract# 2121. [2] Strom, R.G. et al., (2008) *Science, 321*, 79-81. [3] Strom, R.G. et al., (2011) *PSS, 59*, 1960-1967. [4] Robbins, S.J. & B.M. Hynek, (2012) *JGR Planets*, 117. [5] Michael, G.G. & G. Neukum, (2010) *EPSL, 294*, 223-229. [6] Neukum, G. et al., (2001) *PSS, 49*, 1507-1521. [7] Le Feuvre, M. & M.A. Wieczorek, (2011) *Icarus, 214*, 1-20. [8] Ferrari, S. et al, (2015) *Geol. Soc., London, Spec. Pubs.* 401.1: 159-172.